

## Lasing characteristics at different band edges in GaN photonic crystal surface emitting lasers

S. W. Chen, T. C. Lu, Y. J. Hou, T. C. Liu, H. C. Kuo, and S. C. Wang

Citation: *Applied Physics Letters* **96**, 071108 (2010); doi: 10.1063/1.3313947

View online: <http://dx.doi.org/10.1063/1.3313947>

View Table of Contents: <http://scitation.aip.org/content/aip/journal/apl/96/7?ver=pdfcov>

Published by the [AIP Publishing](#)

---

### Articles you may be interested in

[GaN-based surface-emitting laser with two-dimensional photonic crystal acting as distributed-feedback grating and optical cladding](#)

*Appl. Phys. Lett.* **97**, 251112 (2010); 10.1063/1.3528352

[Room temperature photonic crystal band-edge lasing from nanopillar array on GaN patterned by nanosphere lithography](#)

*J. Appl. Phys.* **107**, 063104 (2010); 10.1063/1.3353974

[Characteristics of GaN-based photonic crystal surface emitting lasers](#)

*Appl. Phys. Lett.* **93**, 111111 (2008); 10.1063/1.2986527

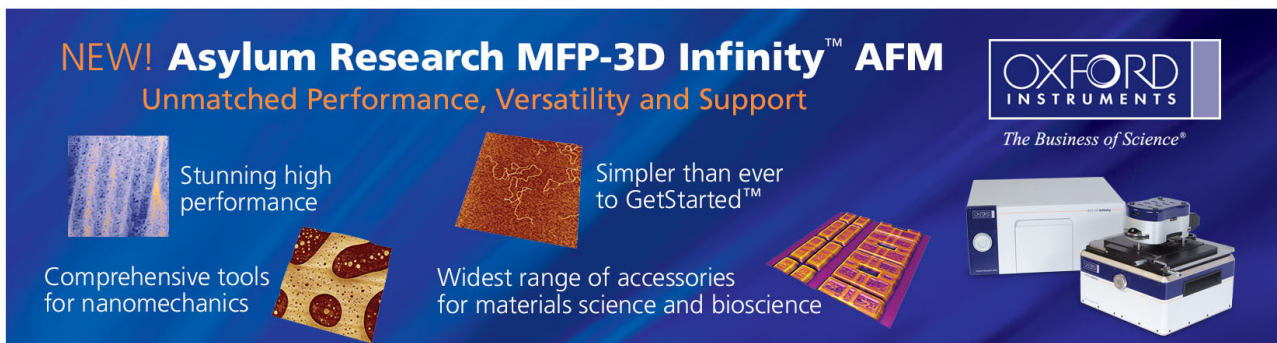
[GaN-based two-dimensional surface-emitting photonic crystal lasers with Al N Ga N distributed Bragg reflector](#)

*Appl. Phys. Lett.* **92**, 011129 (2008); 10.1063/1.2831716

[Butt-end fiber coupling to a surface-emitting -point photonic crystal band edge laser](#)

*Appl. Phys. Lett.* **90**, 171115 (2007); 10.1063/1.2732835

---

The advertisement features a dark blue background with white and orange text. At the top left, it reads 'NEW! Asylum Research MFP-3D Infinity™ AFM' in large white letters, with 'Unmatched Performance, Versatility and Support' in orange below it. To the right is the Oxford Instruments logo, which consists of the word 'OXFORD' in a large, white, serif font above 'INSTRUMENTS' in a smaller, white, sans-serif font, all enclosed in a white rectangular box. Below the logo is the tagline 'The Business of Science®'. The main body of the ad contains four columns of text, each accompanied by a small image: 1. 'Stunning high performance' with an image of a blue and white textured surface. 2. 'Simpler than ever to GetStarted™' with an image of a brown, textured surface. 3. 'Comprehensive tools for nanomechanics' with an image of a yellow and brown textured surface. 4. 'Widest range of accessories for materials science and bioscience' with an image of a yellow and brown textured surface. On the right side, there is a photograph of the MFP-3D Infinity AFM instrument, which is a white and blue device with a large lens and a sample stage.

# Lasing characteristics at different band edges in GaN photonic crystal surface emitting lasers

S. W. Chen,<sup>1</sup> T. C. Lu,<sup>1,2,a)</sup> Y. J. Hou,<sup>1</sup> T. C. Liu,<sup>1</sup> H. C. Kuo,<sup>1</sup> and S. C. Wang<sup>1</sup>

<sup>1</sup>Department of Photonics and Institute of Electro-Optical Engineering, National Chiao-Tung University, Hsinchu 300, Taiwan

<sup>2</sup>Institute of Lighting and Energy Photonics, National Chiao-Tung University, Tainan County 711, Taiwan

(Received 4 December 2009; accepted 18 January 2010; published online 17 February 2010)

We have investigated the lasing characteristics of GaN-based two-dimensional photonic crystal surface emitting lasers (PCSELs) with different PC lattice constants by using angled resolved spectroscopy. Due to the Bragg diffraction theory, normalized frequency of lasing wavelength of PCSELs can be exactly matched with three distinct band-edge frequencies ( $\Gamma_1$ , K2, and M3) in the photonic band diagram. The three band-edge frequencies ( $\Gamma_1$ , K2, and M3) have different emission angles corresponding to the normal direction of the sample ( $0^\circ$ ,  $29^\circ$ , and  $59.5^\circ$ ). © 2010 American Institute of Physics. [doi:10.1063/1.3313947]

Photonic crystal, composed of period structures by dielectric or metal materials, can provide multidirectional distributed feedback effects near the band edges<sup>1-5</sup> which could be considered as good candidates for semiconductor lasers, having characteristics of perfect single mode emission over a large area, high output power, and surface emission with narrow divergence angle.<sup>6,7</sup> These two-dimensional (2D) photonic crystal surface emitting lasers (PCSELs) usually consist of a perfect PC lattice and the laser action would happen in those band edges in the photonic band diagram by satisfying the Bragg condition. The surface emission would occur when the vertical diffraction conditions are satisfied. Most of previous PCSELs operated at  $\Gamma_1$  band edge.<sup>8,9</sup> However, further detailed properties of different band-edge modes for PCSELs, e.g., band structures and lasing angles in vertical directions especially for high order band edges have not been reported. In this report, we will demonstrate the lasing characteristics at different band-edge frequencies or high order lasing modes of GaN-based PCSELs with triangular lattice structures which can be reconstructed by using the angular-solved  $\mu$ -PL system. The measured photonic band diagram could map correspondingly to simulated photonic band structure in K-space and each of PC band-edge modes exhibits a different type of wave coupling mechanism according to the Bragg diffraction mechanism which caused specific lasing emission angles.

The reciprocal spaces of triangular lattice are shown in Fig. 1. The diffracted light wave from the PC structure should satisfy the Bragg's law and energy conservation law as followed:

$$K_d = K_i + q_1 K_1 + q_2 K_2 \quad q_{1,2} = 0, \pm 1, \pm 2, \dots \quad (1)$$

$$\omega_d = \omega_i, \quad (2)$$

where  $K_d$  is a  $xy$ -plane wave vector of diffracted light wave;  $K_i$  is a  $xy$ -plane wave vector of incident light wave;  $q_{1,2}$  is the order of coupling;  $\omega_d$  is the frequency of diffracted light wave, and  $\omega_i$  is the frequency of incident light wave. Equation (1) represents the phase-matching condition (or momen-

tum conservation), and Eq. (2) represents the constant-frequency condition (or energy conservation).<sup>9,10</sup> As shown in Fig. 1(a), the first band-edge mode at  $\Gamma$  boundary, termed as  $\Gamma_1$  band edge, is assisted by second order or by higher order diffraction, the diffracted waves in the in-plane direction includes five directions  $60^\circ$ ,  $120^\circ$ ,  $-60^\circ$ ,  $-120^\circ$ , and  $180^\circ$ . Simultaneously, the diffracted light can emit perpendicularly from the PC surface by satisfying the first order Bragg diffraction as shown in Fig. 1(d). Therefore, the PC lasers can operate as surface emitting lasers. Let us first turn our attention to the K boundary. Figures 1(b) and 1(e) show the in-plane and vertical diffraction for the K2 band-edge mode. To satisfy the energy conservation, these diffracted lights with smaller in-plane  $K$  values need to be diffracted to a tilted angle of  $30^\circ$  off to the normal of the PC surface as shown in Fig. 1(e). Therefore, we could expect that the emission angle of K2 mode would be different from that of the  $\Gamma_1$  mode. Similarly, Figs. 1(c) and 1(f) show the more complicated in-plane and vertical diffraction at M3 band-edge mode. In this case, except the in-plane diffracted light, several inclined diffracted lights can exist. The tilted angles of these inclined diffracted lights can be calculated as  $19.47^\circ$ ,  $35.26^\circ$ , and  $61.87^\circ$  off to the normal of the PC surface, respectively.

The PCSEL structure was grown on 2-in. sapphire substrate and consisted of a 25-pair GaN/AlN distributed Bragg

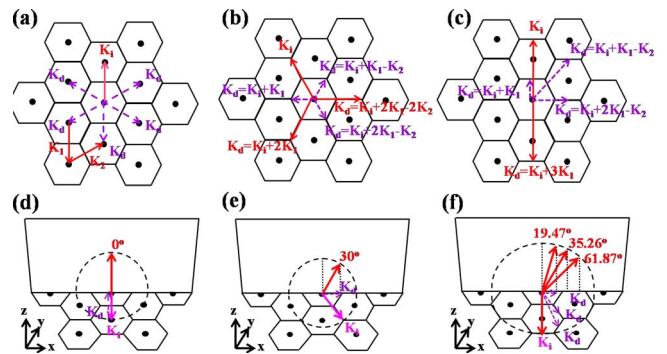


FIG. 1. (Color online) The Bragg diffraction paths of (a)  $\Gamma_1$ , (b) K2, and (c) M3 band-edge modes, respectively. The emission angles on the normal plane of (d)  $\Gamma_1$ , (e) K2, and (f) M3 band-edge modes.

<sup>a)</sup>Author to whom correspondence should be addressed. Electronic mail: timtclu@mail.nctu.edu.tw.

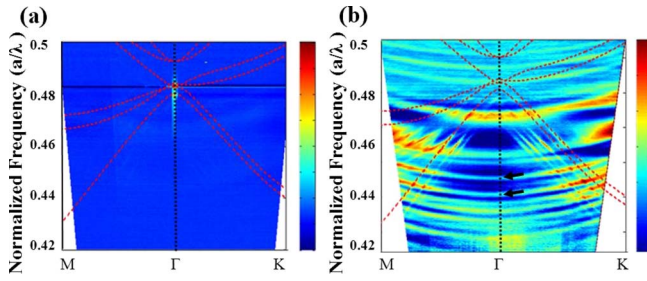


FIG. 2. (Color online) The measured ARPL diagram near the  $\Gamma_1$  mode [(a) pumped by YVO4 pulse laser; (b) pumped by He-Cd laser], the red dashed lines represent the calculated photonic band dispersion curves.

reflector (DBR), a n-GaN layer of about 560 nm, ten pairs of InGaN/GaN multiple quantum wells, and a p-GaN layer of about 200 nm. The PC structure is fabricated on the surface by electron-beam (e-beam) lithography and the etched depth is about 400 nm by using inductively coupled plasma system. The diameter of the whole PC region is about 50  $\mu\text{m}$ , where the hexagonal PC lattice constants are ranging from 190 to 260 nm, and the  $r/a$  ratios are between 0.18 and 0.3. The schematic PCSEL structure and the detailed structural parameters can be found in our previous reports.<sup>11,12</sup> The angle-resolved photoluminescence (ARPL) system has the 325 nm CW He-Cd laser beam or the 355 nm pulse YVO4 laser beam as the optical pumping lasers which are incident onto the PCSEL devices obliquely with a spot size of about 50  $\mu\text{m}$  to cover the whole PC pattern. A fiber with a core radius of 600  $\mu\text{m}$  is used to collect the out-of-plane emission signal from the sample surface by rotated the fiber on a rotational arm. The resolutions of the spectral meter and rotation angle ( $\theta$ ) are 0.7  $\text{\AA}$  and 0.5°, respectively.

The normalized lasing frequencies ( $a/\lambda$ ) of PCSEL devices with different lattice constants can be grouped into three values of 0.48, 0.56, and 0.59, corresponding to PCSEL devices with three different PC lattice constants of 190, 210, and 230 nm, respectively. To further investigate the out-of-plane emission characteristics of our GaN-based PCSELS, we measured the light emissions from  $\Gamma$ -K and  $\Gamma$ -M directions to construct the dispersion diagram by using the ARPL system. The in-plane light wave vector  $k$  is related to the polar angle  $\theta$  according to the relation;  $k=(2\pi/\lambda)\sin\theta$ . Figures 2 show the measured dispersion diagram at  $\Gamma_1$  mode pumped by the YVO4 pulse laser and pumped by the He-Cd laser. The dash lines represent the simulated photonic band diagram around  $\Gamma_1$  mode. Since YVO4 pulse laser has higher pumping energy intensity, it can be clearly seen that the PC laser shows the vertical emission near the normal direction to the sample surface in Fig. 2(a). However, except for the lasing peaks, the diffracted lines in this figure cannot be observed clearly due to high intensity of laser peaks. Alternatively, the diffracted pattern can be more clearly revealed in the measured dispersion diagram pumping by CW He-Cd laser, shown in Fig. 2(b). It should be noted that the transverse upward curving lines [indicated by black arrows in Fig. 2(b)] are resulted from the Fabry-Perot effect provided by the vertical device structure of the p-i-n-GaN layers and modulated by the interference of the DBR layers. Besides, the obvious diffraction lines can be observed with narrow line widths in the measured dispersion diagram, which are resulted from the in-plane PC diffraction.<sup>11</sup> In Fig. 2(b), we can observe several groups with different slopes of dif-

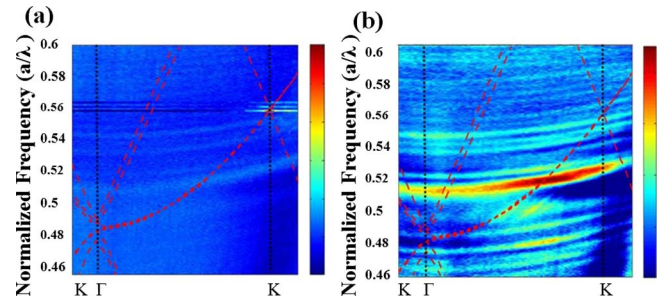


FIG. 3. (Color online) The measured ARPL diagram near the  $K_2$  mode [(a) pumped by YVO4 pulse laser; (b) pumped by He-Cd laser]. The red dashed lines represent the calculated photonic band dispersion curves.

fraction lines in the dispersion diagram. The diffraction lines with different slopes represent different dispersion modes, which can be well matched to calculated dispersion curves shown as dashed lines. The parallel diffraction lines with the same slope represent different guide modes in the in-plane direction. Though several band edges would appear in the calculated dispersion curves as shown in Fig. 2(a), only one dominant lasing peak was observed at the second lowest band-edge mode and one small peak was observed at the lowest band-edge mode due to that the optical fields cover larger gain regions around the PC holes for the two lowest  $\Gamma_1$  band-edge modes in comparison to the two higher order  $\Gamma_1$  band-edge modes.

Figures 3 show the measured ARPL diagrams of another PCSEL device with different PC structure near the  $K_2$  modes along the  $\Gamma$ -K direction. Figure 3(a) shows lasing peaks in the ARPL diagram by using YVO4 pulse laser pumping. In addition, the ARPL diagram in Fig. 3(b) was obtained by using CW He-Cd laser pumping. The emission angle of lasing beam was about 29° off from the normal along the  $\Gamma$ -K direction, which was quite matched to the estimated value (30°) shown in Fig. 1(e). In addition, we measured another PCSEL device exhibited characteristics of  $M_3$  band-edge mode along the  $\Gamma$ -M direction. The measured dispersion diagrams pumped by YVO4 pulse laser and by He-Cd laser are shown in Figs. 4(a) and 4(b), respectively. The lasing peaks can be clearly seen in Fig. 4(a). The emission angle of lasing beam was about 59.5° off from the normal along the  $\Gamma$ -K direction, which was also quite matched to one of the estimated values (61.87°) shown in Fig. 1(f). Only one emission angle was obtained which could be due to that we only measured the ARPL diagram along one  $\Gamma$ -M direction.

Figure 5 shows the divergence angles of  $\Gamma_1$ ,  $K_2$ , and  $M_3$  band-edge modes on the normal plane from the sample sur-

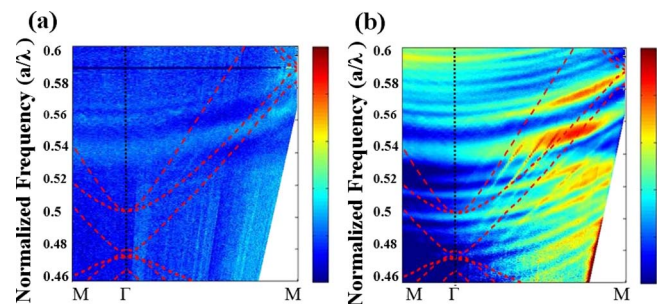


FIG. 4. (Color online) The measured ARPL diagram near the  $M_3$  mode [(a) pumped by YVO4 pulse laser; (b) pumped by He-Cd laser]. The red dashed lines represent the calculated photonic band dispersion curves.



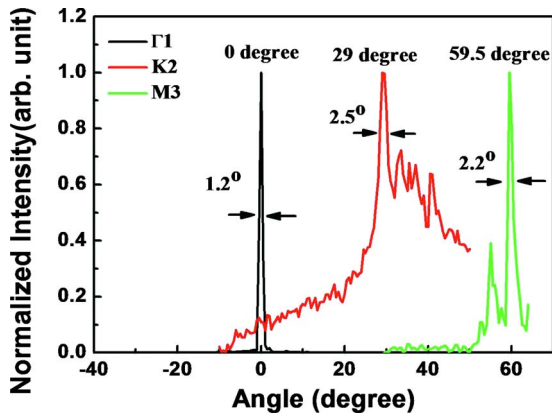


FIG. 5. (Color online) The emission angles and divergence angles of  $\Gamma_1$ , K2, and M3 band-edge modes on the normal plane from the sample surface.

face despite the measurements were along different directions. The lasing emission angles are ( $0^\circ$ ,  $29^\circ$ , and  $59.5^\circ$ ) and the divergence angles of laser beams are ( $1.2^\circ$ ,  $2.5^\circ$ , and  $2.2^\circ$ ) for ( $\Gamma_1$ , K2, and M3) band-edge modes, respectively. The minor peaks at K2 and M3 modes might be due to other guided modes propagated in the GaN and sapphire substrate. Since the high order band-edge modes such as K2 and M3 of photonic crystal lasers require higher threshold gains, the pumping is so intense that the other guided modes could be appeared. Nevertheless, the dominant mode and the divergence angle can be properly identified. It should be noted that the measured emission angles might have some offset values (about  $1^\circ$  to  $2^\circ$ ) due to the alignment difficulties in the ARPL system. However, from the above observation of our PCSEL devices, not only the higher band-edge modes were determined but their characteristics can be properly matched to the Bragg diffraction mechanism in 2D PC structure.

The GaN-based 2D PCSELS are fabricated and measured. Normalized frequency of investigated PC lasing wavelength can be corresponding to three band-edge frequencies ( $\Gamma_1$ , K2, and M3), which indicates the lasing action

can only occur at specific band edges. According to the Bragg diffraction theory and the angle-resolved PL diagrams, it further proved the existence of lasing modes at different band edge ( $\Gamma_1$ , K2, and M3) by mapping the diffraction patterns with band structures. The three band-edge frequencies ( $\Gamma_1$ , K2, and M3) have different emission angles at ( $0^\circ$ ,  $29^\circ$ , and  $59.5^\circ$ ) normal to the sample surface, respectively. Besides, the divergence angles for  $\Gamma_1$ , K2, and M3 band-edge modes are about ( $1.2^\circ$ ,  $2.5^\circ$ , and  $2.2^\circ$ ).

The authors gratefully acknowledge Professor Min-Hsiung Shih at National Chiao-Tung University (NCTU) in Taiwan for his fruitful discussion. This work is supported by the National Nanotechnology Program of Taiwan, R.O.C., and the MOE ATU program and, in part, by the National Science Council of the Republic of China under Contract No. NSC98-3114-M-009-001.

<sup>1</sup>E. Yablonovitch, *Phys. Rev. Lett.* **58**, 2059 (1987).

<sup>2</sup>S. John, *Phys. Rev. Lett.* **58**, 2486 (1987).

<sup>3</sup>M. Meier, A. Mekis, A. Dodabalapur, A. Timko, R. E. Slusher, J. D. Joannopoulos, and O. Nalamasu, *Appl. Phys. Lett.* **74**, 7 (1999).

<sup>4</sup>M. Imada, S. Node, A. Chutinan, and T. Tokuda, *Appl. Phys. Lett.* **75**, 316 (1999).

<sup>5</sup>M. Notomi, H. Suzuki, and T. Tamamura, *Appl. Phys. Lett.* **78**, 1325 (2001).

<sup>6</sup>K. McGroddy, A. David, E. Matioli, M. Iza, S. Nakamura, S. DenBaars, J. S. Speck, C. Weisbuch, and E. L. Hu, *Appl. Phys. Lett.* **93**, 103502 (2008).

<sup>7</sup>H. Matsubara, S. Yoshimoto, H. Saito, Y. Jianglin, Y. Tanaka, and S. Noda, *Science* **319**, 445 (2008).

<sup>8</sup>K. Sakai, E. Miyai, T. Sakaguchi, D. Ohnishi, T. Okano, and S. Noda, *IEEE J. Sel. Areas Commun.* **23**, 1335 (2005).

<sup>9</sup>M. Imada, A. Chutinan, S. Noda, and M. Mochizuki, *Phys. Rev. B* **65**, 195306 (2002).

<sup>10</sup>F. S. Diana, A. David, I. Meinel, R. Sharma, C. Weisbuch, S. Nakamura, and P. M. Petroff, *Nano Lett.* **6**, 1116 (2006).

<sup>11</sup>T. C. Lu, S. W. Chen, L. F. Lin, T. T. Kao, C. C. Kao, P. Yu, H. C. Kuo, and S. C. Wang, *Appl. Phys. Lett.* **92**, 011129 (2008).

<sup>12</sup>T. C. Lu, S. W. Chen, T. T. Kao, and T. W. Liu, *Appl. Phys. Lett.* **93**, 111111 (2008).